Mechanical Strength of Sn-3.5Ag-Based Solders and Related Bondings

CHIANG-MING CHUANG,[1] PO-CHENG SHIH,[1] and KWANG-LUNG LIN[1,2]

1.—Department of Materials Science and Engineering, National Cheng-Kung University, Tainan, Taiwan 701, Republic of China. 2.—E-mail: matkllin@mail.ncku.edu.tw

The tensile strengths of bulk solders and joint couples of Sn-3.5Ag-0.5Cu, Sn-3.5Ag-0.07Ni, and Sn-3.5Ag-0.5Cu-0.07Ni-0.01Ge solders and the shear strengths of ball grid array (BGA) specimens, solder-ball-attached Cu/Ni/Au metallized substrates were investigated. The tensile strength of the bulk is degraded by thermal aging. The Ni-containing solder exhibits lower tensile strength than Sn-3.5Ag-0.5Cu after thermal aging. However, the Ni-containing solder joints show greater tensile strength than the Cu/Sn-3.5Ag-0.5Cu/Cu joint. Fracture of the solder joint occurs between the intermetallic compound (IMC) and the solder. The shear strength and fracture mechanism of BGA specimens are the same regardless of solder composition.

Key words: Sn-3.5Ag based solders, tensile strength, solder joints

INTRODUCTION

The Sn-Ag-based Pb-free solder provides better mechanical properties, creep resistance, thermomechanical fatigue behavior, and solderability on copper and copper alloys than the Sn-Pb solder.[1] Among these, the ternary Sn-Ag-Cu solder, of which the eutectic temperature is 217°C,[2–6] has been recommended as a potential candidate as a Pb-free solder. The eutectic composition lies in the range of Sn-(3.2–4.7)wt.% Ag-(0.5–1.7)wt.%Cu.

Controlling the growth of the interfacial intermetallic compound (IMC) formed between the metallized substrate and the solder is of importance in soldering because the brittle interfacial IMC can affect the reliability of the solder joint.[7] Previous studies[8,9] indicated that Cu_6Sn_5 was the major IMC formed between the solder and the Cu substrate. Extensive aging at high temperature may result in the formation of a Cu_3Sn layer as the first formed Cu_6Sn_5 layer retards the diffusion of Sn.[10]

Fractional additions of extra elements were investigated for modifying the characteristics of the Sn-Ag-Cu solder. It was shown[11–13] that Ni, Co, Ti, Mn, and Fe added to the Sn-Ag-Cu solder could increase the tensile strength of the bulk solder. Furthermore, Ni and Co additions gave rise to a Sn-Cu-Ni and Sn-Cu-Co reaction layer at the interface of the Cu/solder that also increases the joint strength. On the other hand, Ge may be an interesting alloy element as far as mechanical properties are concerned. The addition of Ge improves the mechanical properties and lowers the dross formation of the solder.[14]

The purpose of the present work was to investigate the effect of Ni and Ge additions on tensile properties of the Sn-Ag-based solder. The shear strengths of the Sn-Ag-Cu ball grid array (BGA) solder balls and of the solder joint were also investigated to explore the influence of Ni and Ge addition.

EXPERIMENTAL PROCEDURE

The Sn-3.5Ag-0.5Cu, Sn-3.5Ag-0.07Ni, and Sn-3.5Ag-0.5Cu-0.07Ni-0.01Ge (in wt.%) solders were melted at 260°C and cast into a metal mold to achieve a rapidly solidified microstructure. The as-cast bulk materials were machined to give a tensile specimen with gauge length of 20-mm long × 5-mm wide × 2-mm thick, as shown in Fig. 1a. The tensile test was conducted for the as-cast specimens and for specimens thermally aged at 150°C for 4 h. The tensile test was performed at room temperature at an initial strain rate of $8.3 \times 10^{-4}\ s^{-1}$ in the bulk material.

The Cu/solder/Cu joint (Fig. 1b) specimens for tensile test were prepared by dipping two Cu rods (ϕ = 2 mm) into a solder bath (240°C for 15 sec) to

(Received June 5, 2003; accepted July 29, 2003)

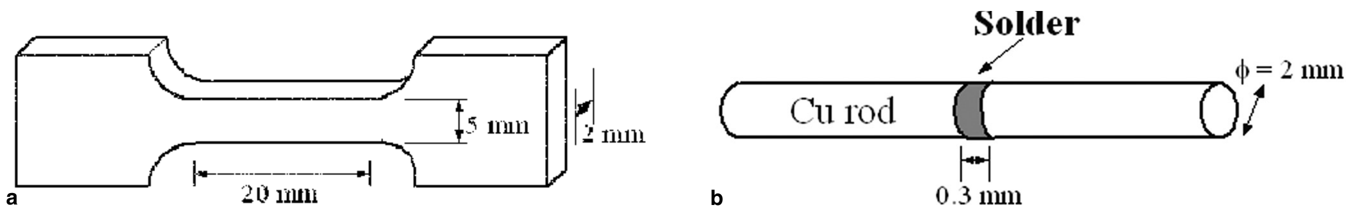

Fig. 1. The schematic configuration of the tensile specimen: (a) dimension of bulk tensile specimen and (b) dimension of solder joint tensile specimen.

produce a 0.3-mm-thick solder joint. The jointing surface of the Cu rod was cleaned with 5wt.%NaOH and 10vol.%HNO_3 solutions. Soldering was performed with the aid of a commercial, rosin mildly activated flux. The solder joint was heat treated at 150°C for 0–1,150 h before the tensile test. The tensile test of the joint specimen was also carried out at room temperature and at an initial strain of 5.5×10^{-2} s^{-1}.

The Sn-3.2Ag-0.5Cu and Sn-3.5Ag-0.5Cu-0.07Ni-0.01Ge solder balls, 760 μm in diameter, were reflowed on the Cu/Ni/Au metallized substrate for the shear test. The reflow experiment was performed in an infrared ray furnace. The reflow profile consists of activation at 170°C and a peak temperature of 240°C for 30 sec. The height of the shear blade is 20 μm from the BGA substrate, and the shear speed is 100 μm/sec. The solder-ball-attached BGA specimen was thermally aged at 150°C for 0–1,000 h prior to the shear test.

The specimens were polished with 0.3-μm Al_2O_3 powder and were etched with 5% HCl-95% C_2H_5OH solution for microstructural investigation by optical microscopy, scanning electron microscopy (SEM), or energy dispersive x-ray analysis (EDX). The excessive solders on the Cu and BGA substrates were removed with a 30% HNO_3-70% C_2H_5OH solution to reveal the IMC morphology.

RESULTS AND DISCUSSION

Microstructure and Tensile Strength of Bulk Materials

The as-cast and thermally aged (150°C for 4 h) microstructures of Sn-3.5Ag-0.5Cu, Sn-3.5Ag-0.07 Ni, and Sn-3.5Ag-0.5Cu-0.07Ni-0.01Ge solders are shown in Fig. 2. The typical microstructure of the Sn-Ag-based solder includes the darker and network regions (eutectic β-Sn + Ag_3Sn) and the dendritic regions (primary β-Sn). Figure 2a and b shows that the fraction of the eutectic region in Sn-3.5Ag-0.5Cu is higher than that in the other two solders. The Sn-3.5Ag-0.07Ni consists of the lowest fraction of the eutectic region among the three solders. Heat treatment did not result in prominent variation in microstructure for all three solders. The grain size of the as-cast specimen (Fig. 2) is greater than that of the joint, to be revealed later. This is due to the faster cooling speed of the joint. It was pointed out[15] that the stable Ag_3Sn inhibits the coarsening of the microstructure at high temperature.

Tensile properties of the solders are shown in Fig. 3. Figure 3a shows that the ultimate tensile strength (UTS) of three as-cast solders is approximately the same, with an average magnitude of 46–47 MPa. The average values of yield strength

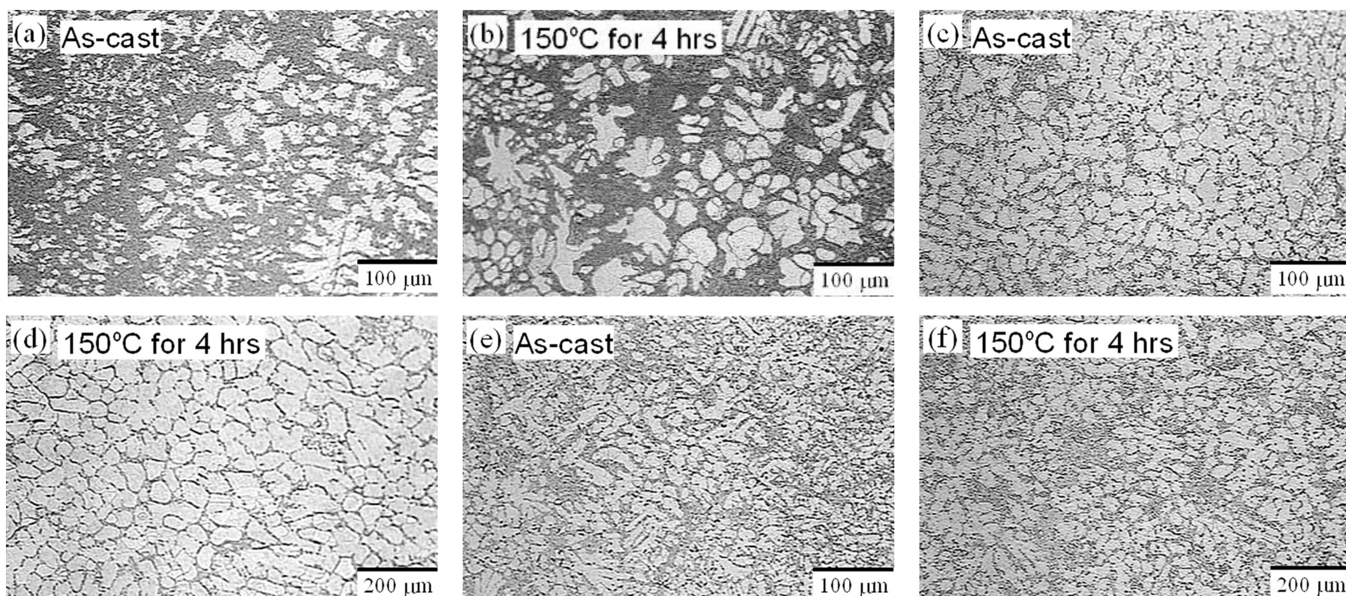

Fig. 2. Metallographs of the as-cast and thermally aged solder: (a) and (b) Sn-3.5Ag-0.5Cu, (c) and (d) Sn-3.5Ag-0.07Ni, and (e) and (f) Sn-3.5Ag-0.5Cu-0.07Ni-0.01Ge.

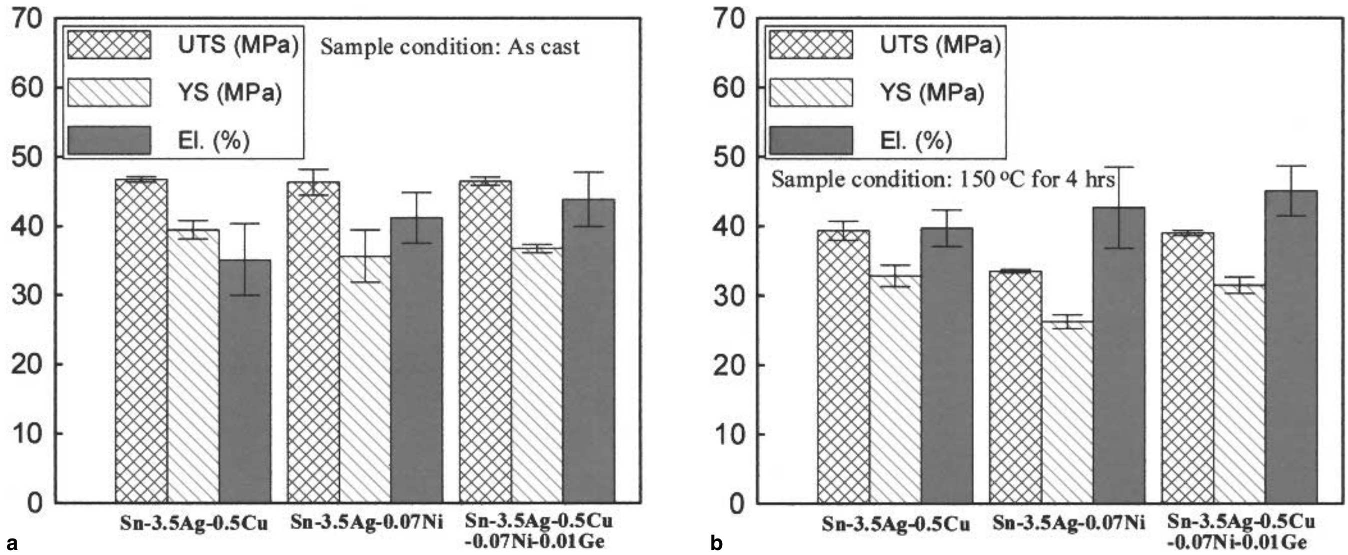

Fig. 3. Tensile properties of the bulk solders: (a) as-cast and (b) thermally aged (at 150°C for 4 h).

(YS) of Sn-3.5Ag-0.5Cu, Sn-3.5Ag-0.07Ni, and Sn-3.5Ag-0.5Cu-0.07Ni-0.01Ge are 39 MPa, 36 MPa, and 37 MPa on average, respectively. The total elongation of the three solders is over 35%. On the other hand, the tensile strength decreases and the elongation increases for all investigated solders after thermal aging at 150°C for 4 h, as shown in Fig. 3b. The UTS and YS of Sn-3.5Ag-0.5Cu are slightly higher than Sn-3.5Ag-0.5Cu-0.07Ni-0.01Ge and Sn-3.5Ag-0.07Ni after heat treatment. This behavior is believed to be caused by the higher content of solute Ag, Cu, Ni, and Ge in the β-Sn of as-cast specimens. The extent of strength variation of the Sn-3.5Ag-0.07Ni solder is the most prominent among the three solders. This is ascribed to the larger fraction of the primary β-Sn phase in the Sn-3.5Ag-0.07Ni solder (Fig. 2). The lowering of the solute content in the primary β-Sn phase will lower the mechanical strength yet increase plastic deformation.

Microstructure of the Solder Joint and Ball Grid Array Specimen

Figure 4 presents the cross-sectional SEM micrograph of as-dipped joint specimens. It is seen that the thickness of the interfacial IMC layer formed with Sn-3.5Ag-0.07Ni and Sn-3.5Ag-0.5Cu-0.07Ni-0.01Ge solders is greater than that formed with the Sn-3.5Ag-0.5Cu solder. This difference in IMC thickness is due to the enhancement in the IMC growth by Ni. The involvement of Ni in the IMC formation provides a vacant 3-d orbital that accelerates the interaction among the constituent elements of the IMC. The relatively thin, interfacial IMC formed in the Cu/Sn-3.5Ag-0.5Cu/Cu joint specimen is scallop-shaped Cu_6Sn_5 as observed in previous studies.[1,16–18] On the other hand, the sponge-shaped interfacial IMC was formed for the other two Ni-containing solder joint specimens, as shown in Fig. 4b and c. The interfacial IMC formed in Cu/Sn-3.5Ag-0.07Ni/Cu and Cu/Sn-3.5Ag-0.5Cu-0.07Ni-0.01Ge/Cu specimens was identified[19] as $(Cu,Ni)_6Sn_5$. Nickel is the major influential factor that enhances the interfacial reaction and, thus, the growth of the interfacial IMC. A previous study[19] indicated that the $(Cu,Ni)_6Sn_5$ layer could be a satisfactory diffusion barrier to prevent Sn and Cu from interdiffusion upon aging. Figure 5 further illustrates that the thickness of the interfacial IMC of the Cu/3.5Ag-0.5Cu/Cu specimen grew, and a Cu_3Sn IMC layer formed between Cu and Cu_6Sn_5 after aging, as shown in Fig. 5a. How-

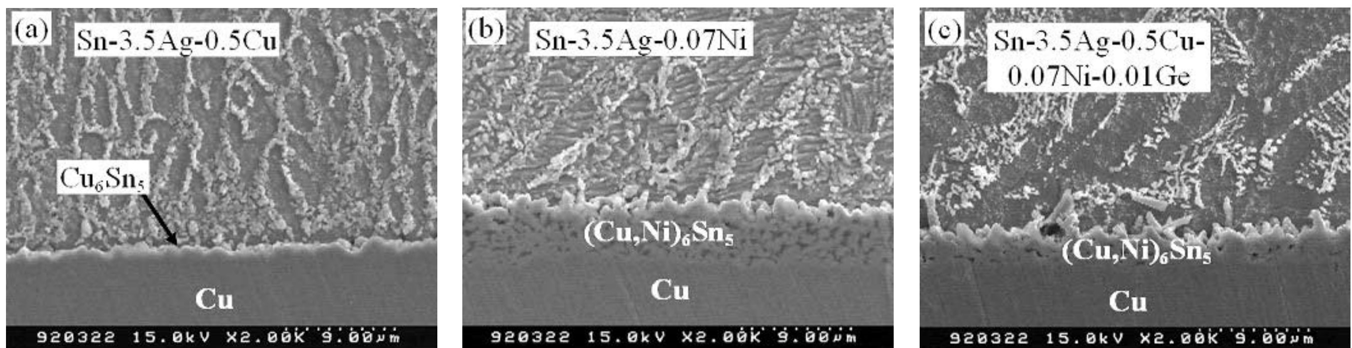

Fig. 4. The feature of the interfacial IMC formed between the solder and the Cu substrate in the as-dipped joint specimen (cross section, dipping temperature: 240°C): (a) Sn-3.5Ag-0.7Cu, (b) Sn-3.5Ag-0.07Ni, and (b) Sn-3.5Ag-0.5Cu-0.07Ni-0.01Ge.

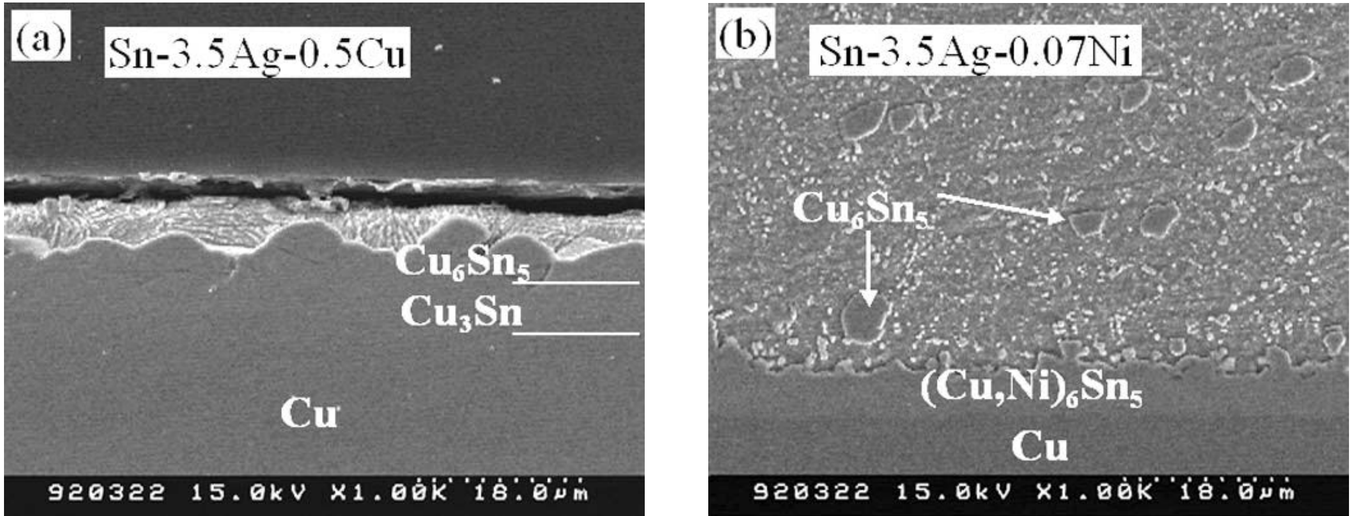

Fig. 5. The feature of the interfacial IMC formed between the solder and the Cu substrate in the joint specimen after aging at 150°C for 1,150 h: (a) Sn-3.5Ag-0.7Cu and (b) Sn-3.5Ag-0.07Ni.

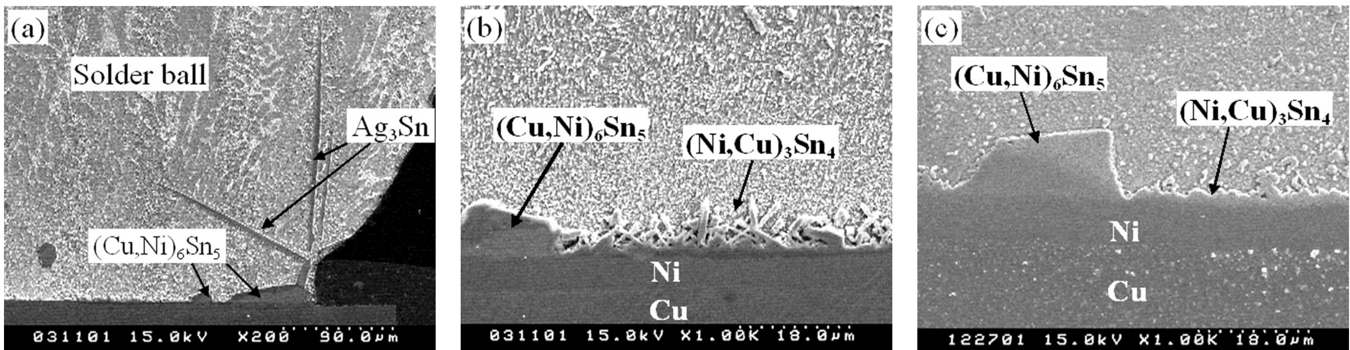

Fig. 6. Cross section of the interfacial IMC formed at the interface of the BGA specimen of the Sn-3.5Ag-0.5Cu-0.07Ni-0.01Ge solder: (a) as-reflowed (low magnification), (b) as-reflowed (high magnification), and (c) thermally aged at 150°C for 1,150 h.

ever, Fig. 5b shows that the thickness of the interfacial IMC of the Cu/Sn-3.5Ag-0.07Ni/Cu specimen did not exhibit an observable change after long-time thermal aging.

The cross section of the as-reflowed and thermally aged BGA specimen is shown in Fig. 6. The morphologies of the interfacial layer are similar for the Sn-3.2Ag-0.5Cu and Sn-3.5Ag-0.5Cu-0.07Ni-0.01Ge solder balls. Figure 6a and b shows that the interfacial IMCs have three types of appearance: plate-shaped, lump-shaped, and thin-layer IMCs. The result of EDX analysis was that the plate-shaped IMC is Ag_3Sn (Fig. 6a), the lump-shaped IMC is $(Cu,Ni)_6Sn_5$, and the thin-layer IMC is $(Ni,Cu)_3Sn_4$. These observations suggest that Cu and Sn of the solder form the Cu-Sn IMC at the interface upon reflow, while Ni participates and accelerates this reaction to form the lump-shaped IMC. Figure 6c further shows the variation in morphology of the IMC in the BGA specimen upon aging at 150°C for 1,000 h. The shape of the $(Ni,Cu)_3Sn_4$ layer becomes smooth after aging without an observable increase in thickness. This result suggests that the Ni is difficult to react with Sn upon aging. The $(Ni,Cu)_3Sn_4$ layer becomes a diffusion barrier to retard the interdiffusion of Sn and Cu.

Tensile Properties of the Joint Specimen

The tensile strengths of the Cu/solder/Cu joints were investigated with respect to aging time at 150°C, as illustrated in Fig. 7. The Sn-3.5Ag-0.07Ni solder joints exhibit the highest tensile strength among the as-dipped specimens. Thermal aging tends to decrease the tensile strength of the three solder joints until it reaches a relatively constant value. The decrease in tensile strength is ascribed to the growth in grain size of the solder upon aging. The tensile values of the thermally aged Sn-3.5 Ag-0.07Ni and the Sn-3.5Ag-0.5Cu-0.07Ni-0.01Ge joints are similar in magnitude but are higher than that of the Sn-3.5Ag-0.5Cu joints. The fracture surface observation, not presented, shows characteristic ductile dimples. Figure 8 presents the cross section of fractured joint specimens. The dimple consisted of the remaining solder and the uncovered IMC at the bottom of the dimple. It is likely that the fracture initiated at the interface between the solder and the interfacial IMC. The tensile fracture surface of the bulk materials (Fig. 3) shows that the strength of the Ni-containing solder is weaker than that of the Sn-3.5Ag-0.5Cu solder. However, the joint strength of the Cu/Sn-3.5Ag-0.07Ni/Cu and

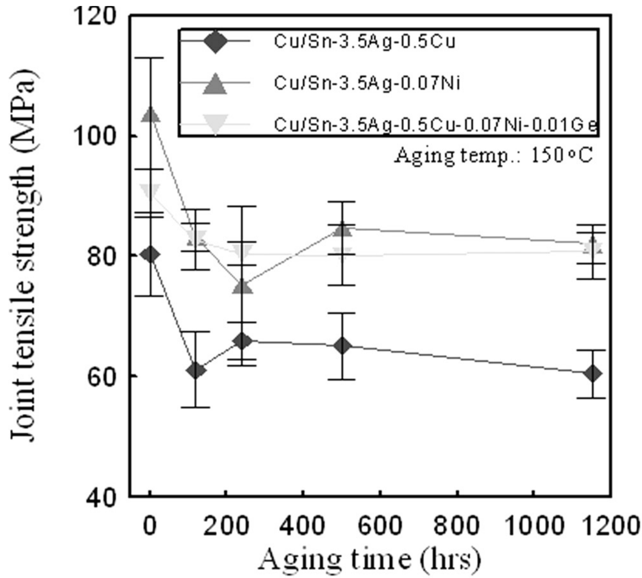

Fig. 7. The tensile strength of various Cu/solder/Cu joints.

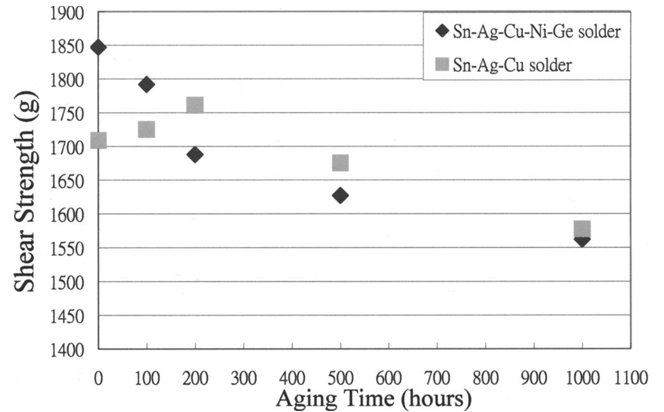

Fig. 9. Shear strength of solder balls on the BGA specimen, thermally aged at 150°C for various durations.

Cu/Sn-3.5Ag-0.5Cu-0.07Ni-0.01Ge/Cu specimens is greater than that of the Cu/Sn-3.5Ag-0.5Cu/Cu specimen. This suggests that the adhesion strength between the solder and the Ni-containing IMC, the $(Ni,Cu)_3Sn_4$ or $(Cu,Ni)_6Sn_5$, is higher than that between the solder and the Cu_6Sn_5 layer formed with the Sn-3.5Ag-0.5Cu solder.

Shear Properties of the Ball Grid Array Sample

Thermal aging tends to degrade the shear strength of the solder-ball attachment (Fig. 9). The shear strength decreases from 1,700 to 1,850 g of as-reflowed BGA specimens to 1,560 to 1,580 g after thermal aging at 150°C for 1,000 h. The degradation of the shear strength after aging could be ascribed to the variation of solute elements in the primary β-Sn phase. Meanwhile, the shear strength of Sn-3.5Ag-0.5Cu and Sn-3.5Ag-0.5Cu-0.07Ni-0.01Ge BGA specimens is approximately the same. The cross section of the fractured BGA specimen shows that the fracture occurs within the solder as represented by the as-reflowed Sn-3.5Ag-0.5Cu BGA specimen (Fig. 10). These observations indicate that the bonding strength between the solder and IMC or the IMC and Ni layer is adequate to withstand the shear force applied during the shear test and is greater than the shear strength of the solders. It is noted that the

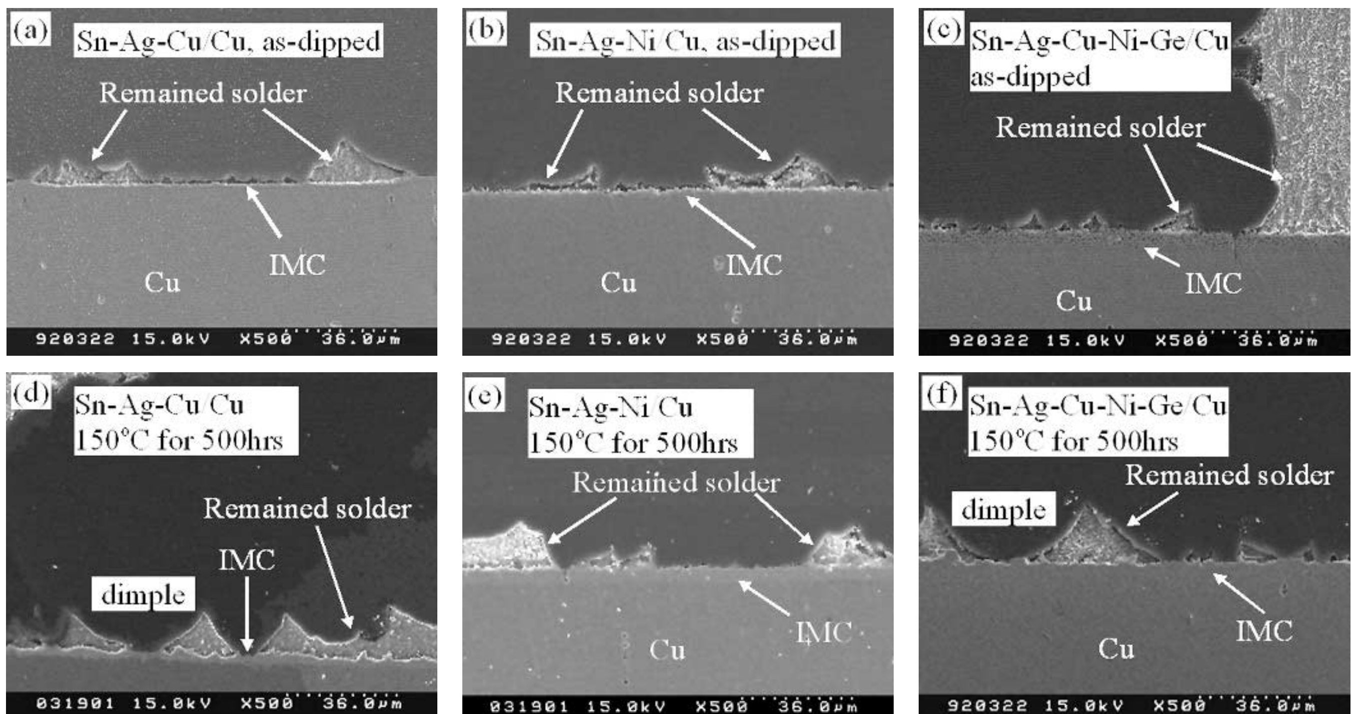

Fig. 8. Cross section of the failure joint specimens after tensile test: (a) as-dipped Sn-3.5Ag-0.5Cu/Cu, (b) as-dipped Sn-3.5Ag-0.07Ni/Cu, (c) as-dipped Sn-3.5Ag-0.5Cu-0.07Ni-0.01Ge/Cu, (d) aged Sn-3.5Ag-0.5Cu/Cu, (e) aged Sn-3.5Ag-0.07Ni/Cu, and (f) aged Sn-3.5Ag-0.5Cu-0.07Ni-0.01Ge/Cu.

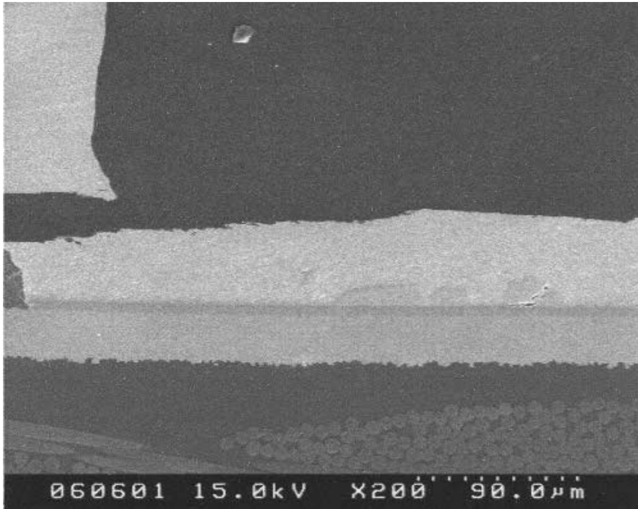

Fig. 10. Cross section of the as-reflowed BGA specimen of the Sn-3.5Ag-0.5Cu solder ball after the shear test.

tensile strength of Cu/Sn-3.5Ag-0.5Cu is lower than that of Cu/Sn-3.5Ag-0.5Cu-0.07Ni-0.01Ge. But, the shear strength is slightly in the opposite order after 200 h of aging. The shear fracture occurs within the solder for all tests, as seen in Fig. 10, while the tensile failure occurs both in the solder and at the solder/IMC interface but is initiated at the interface, as discussed earlier. This is ascribed to the higher bonding strength between the Ni-containing IMC and solder than without Ni.

CONCLUSIONS

The tensile strengths are approximately the same for the investigated as-cast solders. Yet, the tensile strength of the solders is degraded by thermal aging and exhibit the decreasing order of strength of Sn-3.5Ag-0.5Cu, Sn-3.5Ag-0.5Cu-0.07Ni-0.01Ge, and Sn-3.5Ag-0.07Ni. The as-reflowed Cu/solder/Cu joint forms a thin, scallop Cu_6Sn_5 for the Sn-3.5Ag-0.5Cu solder yet a thick $(Cu,Ni)_6Sn_5$ and $(Ni,Cu)_3Sn_4$ for the Ni-containing solder. The Ni-containing IMC did not grow upon aging of the joint, while the Cu_6Sn_5 grew extensively in the Cu/Sn-3.5Ag-0.5Cu/Cu joint. The joints produced with the Ni-containing solder exhibit greater tensile strength than that produced with the Sn-3.5Ag-0.5Cu solder. The fracture of the solder joints upon tensile test occurs between the IMC and the solder. The shear strength and the fracture mechanism of the BGA specimens, with the solder ball attached to the Cu/Ni/Au metallized substrate, are the same regardless of solder composition. The fracture occurs within solder.

ACKNOWLEDGEMENTS

The financial support of this work from the National Science Council of the Republic of China (Taiwan) under Grant No. NSC91-2216-E-006-035 is gratefully acknowledged. The authors also thank Accurus Inc. for supplying the solder balls.

REFERENCES

1. B. Salam, N.N. Ekere, and D. Rajkumar, *2001 Electronic Components and Technology Conf.* (Piscataway, NJ: IEEE, 2001), pp. 471–477.
2. C.M. Miller, I.E. Anderson, and J.F. Smith, *J. Electron. Mater.* 23, 595 (1994).
3. M.E. Loomans and M.E. Fine, *Metall. Mater. Trans. A* 31A, 1155 (2000).
4. K.W. Moon, W.J. Boettinger, U.R. Kattner, F.S. Biancaniello, and C.A. Handwerker, *J. Electron. Mater.* 29, 1122(2000).
5. I. Ohnuma, M. Miyashita, K. Anzai, X. J. Liu, H. Ohtani, R. Kainuma, and K. Ishida, *J. Electron. Mater.* 29, 1137 (2000).
6. K.S. Kim, S.H. Huh, and K. Suganuma, *Mater. Sci. Eng. A* 333, 106 (2002).
7. K.S. Bae and S.J. Kim, *J. Electron. Mater.* 30, 1452 (2001).
8. S. Ahat, M. Sheng, and L. Luo, *J. Mater. Res.* 16, 2914 (2001).
9. T.Y. Lee, W.J. Choi, K.N. Tu, J.W. Jang, S.M. Kuo, J.K. Lin, D.R. Frear, K. Zeng, and J.K. Kivilahti, *J. Mater. Res.* 17, 291 (2002).
10. J.W. Jang, D.R. Frear, T.Y. Lee, and K.N. Tu, *J. Appl. Phys.* 88, 6359 (2000).
11. S.K. Kang et al., *IEEE Trans. Electron. Packaging Manufacturing* 25, 155 (2002).
12. J.K. Park, C.W. Yang, J.S. Ha, C.-U. Kim, E.J. Kwon, S.B. Jung, and C.S. Kang, *J. Electron. Mater.* 30, 1165 (2001).
13. K.S. Kim, S.H. Shih, and K. Suganuma, *Microelectron. Reliab.* 43, 259 (2003).
14. K. Habu, N. Takeda, H. Watanabe, H. Ooki, J. Abe, T. Saito, Y. Taniguchi, and H. Yokohama, *Proc. EcoDesign: 1st Int. Symp. on Environmentally Conscious Design and Inverse Manufacturing* (Los Alamitos, CA: IEEE Computer Society, 1999), pp. 606–609.
15. K. Suganuma, S.H. Huh, K. Kim, H. Nakase, and Y. Nakamura, *Mater. Trans. JIM* 42, 286 (2001).
16. K. Zeng and K.N. Tu, *Mater. Sci. Eng. R* 38, 51 (2000).
17. W.K. Choi and H.M. Lee, *J. Electron. Mater.* 28, 1251 (1999).
18. F. Guo, S. Choi, J.P. Lucas, and K.N. Subramanian, *J. Electron. Mater.* 29, 1241 (2000).
19. C.M. Chuang and K.L. Lin, *Int. Symp. on Electronic Material and Packaging*, Kaohsiung, Taiwan, 4–5 December 2002.